Washington University School of Medicine
Digital Commons@Becker

Open Access Publications

1-1-2010

Interdependent roles for accessory KChIP2, KChIP3, and KChIP4 subunits in the generation of Kv4-encoded IA channels in cortical pyramidal neurons

Aaron J. Norris
Washington University School of Medicine in St. Louis

Nicholas C. Foeger
Washington University School of Medicine in St. Louis

Jeanne M. Nerbonne
Washington University School of Medicine in St. Louis

Follow this and additional works at: http://digitalcommons.wustl.edu/open_access_pubs

Part of the Medicine and Health Sciences Commons

Recommended Citation
Norris, Aaron J.; Foeger, Nicholas C.; and Nerbonne, Jeanne M., ,"Interdependent roles for accessory KChIP2, KChIP3, and KChIP4 subunits in the generation of Kv4-encoded IA channels in cortical pyramidal neurons." The Journal of Neuroscience.30,41. 13644-13655. (2010).
http://digitalcommons.wustl.edu/open_access_pubs/235

This Open Access Publication is brought to you for free and open access by Digital Commons@Becker. It has been accepted for inclusion in Open Access Publications by an authorized administrator of Digital Commons@Becker. For more information, please contact engeszer@wustl.edu.

Cellular/Molecular

Interdependent Roles for Accessory KChIP2, KChIP3, and KChIP4 Subunits in the Generation of Kv4-Encoded I_A Channels in Cortical Pyramidal Neurons

Aaron J. Norris, Nicholas C. Foeger, and Jeanne M. Nerbonne
Department of Developmental Biology, Washington University School of Medicine, St. Louis, Missouri 63110

The rapidly activating and inactivating voltage-dependent outward K^+ (Kv) current, I_A, is widely expressed in central and peripheral neurons. I_A has long been recognized to play important roles in determining neuronal firing properties and regulating neuronal excitability. Previous work demonstrated that Kv4.2 and Kv4.3 α-subunits are the primary determinants of I_A in mouse cortical pyramidal neurons. Accumulating evidence indicates that native neuronal Kv4 channels function in macromolecular protein complexes that contain accessory subunits and other regulatory molecules. The K^+ channel interacting proteins (KChIPs) are among the identified Kv4 channel accessory subunits and are thought to be important for the formation and functioning of neuronal Kv4 channel complexes. Molecular genetic, biochemical, and electrophysiological approaches were exploited in the experiments described here to examine directly the roles of KChIPs in the generation of functional Kv4-encoded I_A channels. These combined experiments revealed that KChIP2, KChIP3, and KChIP4 are robustly expressed in adult mouse posterior (visual) cortex and that all three proteins coimmunoprecipitate with Kv4.2. In addition, in cortical pyramidal neurons from mice lacking KChIP3 (KChIP3$^{-/-}$), mean I_A densities were reduced modestly, whereas in mean I_A densities in KChIP2$^{-/-}$ and WT neurons were not significantly different. Interestingly, in both KChIP3$^{-/-}$ and KChIP2$^{-/-}$ cortices, the expression levels of the other KChIPs (KChIP2 and 4 or KChIP3 and 4, respectively) were increased. In neurons expressing constructs to mediate simultaneous RNA interference-induced reductions in the expression of KChIP2, 3, and 4, I_A densities were markedly reduced and Kv current remodeling was evident.

Introduction

The rapidly activating and inactivating voltage-dependent outward K^+ (Kv) current, I_A, is widely expressed in central and peripheral neurons (Rogawski, 1985). I_A has long been recognized to play important roles in determining neuronal firing properties (Connor and Stevens, 1971a,b) and regulating neuronal excitability under normal (Aghajanian, 1985) and pathologic conditions, such as epilepsy (Bernard et al., 2004). Recent studies have also demonstrated that alterations in the functional expression of I_A in dendritic compartments is important for regulating the backpropagation (into dendrites) of action potentials, synaptic potentiation, and dendritic integration (Cai et al., 2004; Makara et al., 2009). Recognition of the many important roles that I_A plays in neuronal processing has focused considerable effort on understanding the mechanisms that determine the functional expression of I_A channels.

Substantial progress has been made in understanding the roles of Kv pore-forming (α) subunits in the generation of I_A. In hippocampal pyramidal and dorsal horn neurons, Kv4.2 α-subunits encode I_A (Chen et al., 2006; Hu et al., 2006), whereas in dorsal root ganglion neurons and hippocampal interneurons, Kv4.3 has been suggested to generate I_A (Bourdeau et al., 2007; Phuket and Covarrubias, 2009). In mouse cortical pyramidal neurons, however, I_A is encoded by Kv4.2, Kv4.3, and Kv1.4 α-subunits (Norris and Nerbonne, 2010). Considerable evidence indicates that neuronal Kv4 channels function in macromolecular complexes that contain accessory subunits and other regulatory molecules (Schulte et al., 2006; Covarrubias et al., 2008; Marionneau et al., 2009). Multiple putative Kv4 accessory subunits have been identified including the following: Kvβ subunits (Aimond et al., 2005), dipeptidyl peptidase (DPP) family members (DPP6 and DPP10) (Nadal et al., 2003; Jerng et al., 2005), MinK/MiRP family members (Roepke et al., 2008), as well as K^+ channel interacting proteins (KChIP1, KChIP2, KChIP3, and KChIP4) (An et al., 2000; Morohashi et al., 2002).

Several previous studies in heterologous expression systems have demonstrated that coexpression of one or more of these Kv channel accessory subunits dramatically alters the properties and functional expression of Kv4-encoded currents (Martens et al., 1999; Radicke et al., 2006; Maffie and Rudy, 2008). Coexpression with one of the KChIPs, for example, results in Kv4 currents that

Received May 13, 2010; revised Aug. 7, 2010; accepted Aug. 12, 2010.

This work was supported by National Institutes of Health Grant NS030676 (J.M.N.), National Eye Institute Institutional Training Grant T32-EY013360 (A.J.N.), and National Heart Lung and Blood Institute Institutional Training Grant T32-HL007275 (N.C.F.). We thank Amy Huntley for the preparation and maintenance of glia cultures, Rebecca Mellor for assistance with quantitative PCR, and Rick Wilson for the maintenance and screening of the mouse lines used in this study. We also thank Dr. Kai-Chien Yang and Dr. Yarimar Carrasquillo for many valuable discussions and for comments on this manuscript. The KChIP3 knock-out mice were kindly provided by Dr. Mark Bowlby (Wyeth Ayerst Pharmaceuticals, Princeton, NJ), and the KChIP2 knock-out mice were provided by Dr. Masa Hoshijima (University of California, San Diego, La Jolla, CA).

Correspondence should be addressed to Jeanne M. Nerbonne, Department of Developmental Biology, Washington University School of Medicine, Campus Box 8103, 660 South Euclid Avenue, St. Louis, MO 63110. E-mail: jnerbonne@wustl.edu.

DOI:10.1523/JNEUROSCI.2487-10.2010

Copyright © 2010 the authors 0270-6474/10/3013644-12$15.00/0

inactivate more slowly and recover from inactivation more quickly than the currents generated by Kv4 α-subunits expressed alone (An et al., 2000). Also, the coexpression of KChIPs markedly increases Kv4-encoded current densities (Shibata et al., 2003). Interestingly, heterologous coexpression of other accessory subunits, such as the DPPs and Kvβs, with Kv4 α-subunits also alters densities and properties of Kv4-encoded currents (Yang et al., 2001; Jerng et al., 2005). Although the many studies conducted in heterologous cells have informed our understanding of the interactions of accessory subunits with Kv4 α-subunits, little is presently known about the functional roles played by accessory subunits in the generation of native neuronal Kv4 channel complexes. A combination of biochemical and molecular genetic tools was exploited in the studies described here to examine directly the functional roles of the KChIPs in regulating/modulating Kv4-encoded currents in (mouse visual) cortical pyramidal neurons.

Materials and Methods

DNA constructs. Plasmids containing the coding sequences for mouse Kv4.2, KChIP2, KChIP3, and KChIP4 were obtained from Open Biosystems. The KChIP4 clone used here encodes the same amino acid sequence as the variant termed KChIP4b (Holmqvist et al., 2002).

Plasmids encoding human microRNA30 (miR30) with substitutions made in the targeting sequence region (miRNA) and a fluorescent protein (see below) were constructed following a previously described approach (Du et al., 2006). Briefly, the miR30 sequence was placed between splice donor and acceptor sequences in an artificial intron. This arrangement allows the miRNA sequence to be spliced away from the transcript, so that a single transcript can be processed to mediate RNA interference (RNAi) and be used for translation to generate the encoded fluorescent protein. The miRNA intron plasmid was assembled by combining the human miR30 sequence from the pPrime system described by Stegmeier et al. (2005) with the chimeric intronic sequence taken from the Promega PCI-Neo vector. The miR30 sequence was placed in the branch region between the 5′ donor site and the 3′ acceptor site of the first intron of the human β-globin gene (Bothwell et al., 1981; Brondyk, 1995). The sequence containing miR30, as well as the exon and intron components, was synthesized to order by CelTek and subsequently cloned into the multicloning site of Clontech N-1 vectors, encoding either the enhanced yellow florescent protein (YFP) or the enhanced cyan florescent protein (CFP) at the Nhe1 and HindIII sites. To generate a red fluorescent version of the vector, the coding sequence was replaced with the sequence coding for the red fluorescent protein tdTomato (Shaner et al., 2004). Individual targeting sequences specific for KChIP2, 3, or 4 were obtained from Open Biosystems in pSM2C vectors or were designed using the RNAI Codex algorithm and shRNA designer tool (Olson et al., 2006) and synthesized (Sigma-Aldrich). Specific targeting hairpins were subsequently cloned into the XhoI and EcoRI sites in the miR30. Multiple targeting sequences for KChIP2, KChIP3, and KChIP4 were screened for effectiveness in reducing the expression of cotransfected target (mouse KChIP2, 3, or 4) when transfected at ratios of 1:1 in HEK-293 cells.

The targeting sequences that proved effective in reducing the expression of the targets were then used in subsequent experiments in neurons. The targeting 22-mer sequences used were as follows: for KChIP2, ATCCATGCAACTCTTTGATAAT, for KChIP3, TCCATGCAGCTGTTTGAGAAC, and for KChIP4, CCCAGAGCAAATTCACCAAGAA. BLAST searches confirmed that none of the targeting sequences for individual KChIPs had sequence homology to the other KChIPs or other known genes. The targeting sequence used for KChIP4 is complementary to both the KChIP4a and 4b splice variants. For control experiments, nontargeting (not complementary to any cDNA sequences in the mouse genome) hairpin sequences were used in the intron miRNA vector in place of the specific targeting hairpins. One control sequence targeted luciferase (Stegmeier et al., 2005) and the other was a scrambled sequence. For experiments, equal amounts of DNA for nontargeting and targeting vectors were transfected into neurons.

Isolation, maintenance, and transfection of cortical pyramidal neurons. Neurons were isolated from the primary visual cortices of postnatal day 6–8 mice using previously described methods (Huettner and Baughman, 1986; Nerbonne et al., 2008). Briefly, each animal was anesthetized with isoflurane and rapidly decapitated. The brain was then removed and the posterior cortex dissected. The tissue containing the full thickness of the visual cortex was then dissected, chopped into small pieces, and incubated at 37°C in Neurobasal medium (Invitrogen) containing papain (66 U/ml) (Worthington Biochemicals) under 95% O_2/5% CO_2 for 30 min. Subsequent to the enzyme treatment, tissues pieces were triturated using fire-polished Pasteur pipettes. Isolated neurons were recovered by centrifugation for 15 min through a bovine serum albumin gradient. Cells were resuspended in Neurobasal medium and plated on previously prepared monolayers of rat cortical astrocytes (Huettner and Baughman, 1986). One hour after plating, Neurobasal medium was replaced with Minimum Essential Medium (Invitrogen) supplemented with 10% fetal bovine serum, 0.3% glucose, and 0.14 mM L-glutamine. Cell cultures were maintained in an incubator with 5% CO_2 at 37°C.

Neurons were transfected using the Amaxa Nucleofector II and the Amaxa mouse hippocampal kit (Lonza) according to the directions from the manufacturer. For transfections, isolated neurons obtained by centrifugation through a bovine serum albumin gradient were resuspended in the solution included in the nucleofection kit plus the miRNA plasmids, subjected to electroporation, and resuspended in medium immediately before plating. Based on fluorescent protein expression, 48 h after transfections ~10–30% of cells were transfected (data not shown).

Human embryonic kidney-293 cell culture and transfection. Human embryonic kidney-293 (HEK-293) cells were maintained in DMEM supplemented with 5% fetal bovine serum, 5% horse serum, and penicillin/streptomycin (Invitrogen) in a 5% CO_2 37°C incubator. HEK-293 cells were transfected using Lipofectamine 2000 (Invitrogen) and were maintained in Opti-MEM (Invitrogen) during the 8 h transfection period.

Electrophysiological recordings. Recordings of whole-cell Kv currents were obtained from pyramidal shaped neurons on the second and third day in culture (~48–72 h after plating) at room temperature (22–23°C). Process growth was limited during the first 3 d in culture, thereby allowing for adequate voltage clamp. Pyramidal shaped neurons expressing the microRNA constructs, as determined by fluorescent protein expression, were selected for recordings. Data were collected using an Axon 1D amplifier (Molecular Devices) interfaced to a personal computer (Dell), using a Digidata 1322 (Molecular Devices) analog-to-digital converter. Pipettes were fabricated from borosilicate glass (WPI) with a Sutter model P-87 horizontal puller (Sutter Instrument). For recordings, the bath solution routinely contained the following (in mM): 140 NaCl, 4 KCl, 2 $CaCl_2$, 2 $MgCl_2$, 10 HEPES, 5 glucose, 0.001 TTX, and 0.1 $CdCl_2$, pH 7.4 and 300 mOsM. The recording pipette solution contained the following (in mM): 135 KCl, 10 HEPES, 5 glucose, 1.1 $CaCl_2$, 2.5 BAPTA, 3 MgATP, and 0.5 NaGTP, pH 7.4 and 300 mOsM. The calculated free Ca^{2+} in this BAPTA-buffered pipette solution was 100 nM (MaxChelator) (Patton et al., 2004). Using this pipette solution, pipette resistances were between 2 and 4 MΩ. All reagents were from Sigma-Aldrich unless otherwise noted.

For all experiments, junction potentials were zeroed before forming pipette–membrane seals. Signals sampled at 100 kHz and low-pass filtered at 10 kHz. Whole-cell Kv currents were evoked in response to 4 s depolarizing voltage steps to potentials between −40 and +40 mV (in 10 mV increments) from a holding potential of −70 mV. Also, a prepulse paradigm, which included a 60 ms step to −10 mV before steps to test potentials from −40 to +40 mV (in 10 mV increments), was used to facilitate the isolation of the rapidly inactivating currents in each cell. Subsequent off-line subtraction of the current records obtained with the prepulse from the current records obtained without the prepulse (in the same cell) allowed the isolation of the rapidly inactivating outward K^+ currents (see Fig. 1).

Data analysis. Data were compiled and analyzed using ClampFit (Molecular Devices), Microsoft Excel, and Prism (GraphPad). Only data from cells with input resistances >300 MΩ and access resistances <15 MΩ were included in the analyses. Membrane capacitances were determined by analyzing the decay phases of capacitive currents elicited by

short (25 ms) voltage steps (±10 mV) from the holding potential (−70 mV). Consistent with the limited outgrowth of processes during the first 3 d in culture, a single exponential was sufficient to describe the decay phases of the capacitive transients. Whole-cell membrane capacitances (C_m) were calculated for each cell by dividing the integrated capacitive transients by the voltage. Input resistances were calculated from the steady-state currents elicited by the same ±10 mV steps (from the holding potential of −70 mV). For each cell, the series resistance was calculated by dividing the time constant of the decay of the capacitive transient by the C_m; the mean (±SEM) series resistance was 5.8 ± 0.1 MΩ ($n = 155$). Series resistances were compensated electronically by >80% in all cells. Voltage errors resulting from uncompensated series resistances, therefore, were small (<2 mV) and were not corrected. The inactivation phases of the Kv currents were analyzed using the following equation: $y = A1e\text{-}t/\tau1 + A2e\text{-}t/\tau2 + A3e\text{-}t/\tau3 + C$, where A1, A2, and A3 are the amplitudes of individual current components (see text), each with a characteristic time constant of decay ($\tau1$, $\tau2$, and $\tau3$), and C is the non-inactivating component (I_{SS}) of the total Kv current (Locke and Nerbonne, 1997a). Statistical analyses were conducted using Prism. The statistical significance of observed differences in current–voltage plots (*IV* plots) was calculated using repeated-measurement ANOVA. The Mann–Whitney test was used to examine the statistical significance of the differences of the mean ± SEM of results from Western blot and quantitative real-time PCR (QRT-PCR) data. The column *t* test was used for statistical analyses of results obtained in the experiments that examined the expression levels of heterologously expressed Kv4.2 and KChIPs.

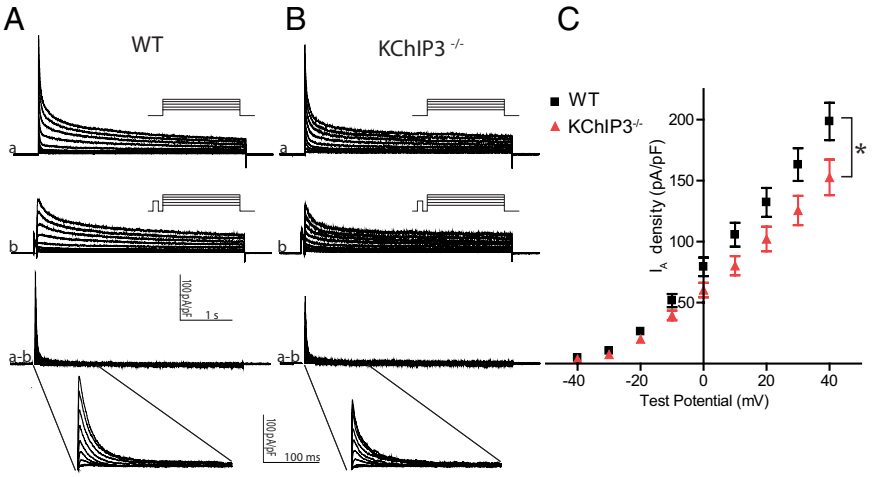

Figure 1. I_A density is reduced in KChIP3 $^{-/-}$ cortical pyramidal neurons. ***A***, ***B***, Whole-cell Kv current recordings were obtained from cortical pyramidal neurons isolated from WT and KChIP3 $^{-/-}$ mice. Representative recordings from WT (***A***) and KChIP3 $^{-/-}$ (***B***) neurons are illustrated. In each cell, Kv currents were elicited by depolarizing voltage steps ranging from −40 to +40 mV in 10 mV increments from a holding potential of −70 mV (a). Recordings were then obtained from the same cell using a prepulse paradigm in which the same depolarizing steps, preceded by a prepulse of 60 ms to −10 mV to selectively inactive I_A, were presented (b). The paradigms are illustrated in the insets. For each cell, currents recorded with the prepulse (b) were subtracted off-line from the control records (a) to isolated I_A (a − b). Similar recordings were obtained from WT ($n = 22$) and KChIP3 $^{-/-}$ ($n = 24$) neurons. ***C***, I_A densities were calculated from the subtracted records, and mean ± SEM I_A densities are plotted. Mean ± SEM I_A densities were modestly, but significantly (*$p < 0.05$), lower in KChIP3 $^{-/-}$, compared with WT, neurons.

Immunoprecipitation and Western blots. For the isolation of tissue for biochemical analyses, mice were anesthetized with isoflurane and rapidly decapitated, and the brains were removed. The posterior (~1 mm) cortex, which contains visual areas, was dissected and flash frozen in liquid nitrogen. Tissue samples were collected from wild-type (WT) C57BL/6 mice and mice (Kv4.2 $^{-/-}$, Kv4.3 $^{-/-}$, KChIP2 $^{-/-}$, and KChIP3 $^{-/-}$) harboring targeted disruptions of the genes encoding Kv4.2 (*Kcnd2*) (Guo et al., 2005; Nerbonne et al., 2008), Kv4.3 (*Kcnd3*) (Niwa et al., 2008), KChIP2 (*Kcnip2*) (Kuo et al., 2001), and KChIP3 (*Kcnip3*) (Alexander et al., 2009). Also, samples from mice (Kv4.2 $^{-/-}$/Kv4.3 $^{-/-}$) generated by breeding Kv4.2 $^{-/-}$ and Kv4.3 $^{-/-}$ animals were used (Norris and Nerbonne, 2010).

For experiments focused on examining the expression of the KChIP and Kv4 proteins, total protein samples from posterior cortices collected from adult (WT, Kv4.2 $^{-/-}$, Kv4.2 $^{-/-}$, Kv4.3 $^{-/-}$/Kv4.3 $^{-/-}$, KChIP2 $^{-/-}$, and KChIP3 $^{-/-}$) mice were prepared using previously described methods (Brunet et al., 2004). Protein concentrations were determined for each sample using a Bio-Rad protein assay kit (Bio-Rad) following the directions from the manufacturer. Equal amounts of proteins were then fractionated by SDS-PAGE and transferred to polyvinylidene fluoride (PVDF) membranes. For immunoblotting, PVDF membranes with bound proteins were incubated in blocking buffer (PBS, 1% Tween, and 5% dry milk) for 1 h at room temperature. Membranes were then incubated overnight at 4°C with primary antibodies against Kv4.2, Kv4.3, or the individual KChIPs (KChIP2, KChIP3, and KChIP4). All primary antibodies were from the University of California, Davis/National Institutes of Health NeuroMab Facility with the exception of the goat anti-KChIP4 antibody from Santa Cruz Biotechnology. Bound primary antibodies were detected using horseradish peroxidase-conjugated rabbit anti-mouse IgG (GE Healthcare) or rabbit anti-goat IgG (Bethyl Labs) and the Durawest chemiluminescence reagent (Pierce). Signals were detected and quantified using the Bio-Rad Chemidoc system and the Quantity One software (Bio-Rad). Blots were then reprobed with primary antibodies against glyceraldehyde 3-phosphate dehydrogenase (GAPDH) (Abcam), transferrin receptor (Invitrogen), or β-tubulin (Sigma-Aldrich) to verify equal protein loading in each lane. For quantification, the signals from the anti-GAPDH, the anti-transferrin receptor, or the anti-β-tubulin antibodies were used to normalize the anti-Kv4 or anti-KChIP signals for each lane on the same blot, as described in the text.

For immunoprecipitations, posterior cortical tissue samples from adult WT and Kv4.2 $^{-/-}$ mice were processed, and immunoprecipitations were conducted using previously described methods (Marionneau et al., 2009). Briefly, the tissues pieces were homogenized in ice-cold lysis buffer: PBS [containing the following (in mM): 136 NaCl, 2.6 KCl, 10 NaH_2PO_4, 1.7 KH_2PO_4, pH 7.4] plus one protease inhibitor mixture tablet (Roche) and Triton X-100 (1%). After 15 min rotation at 4°C, 4 mg of the soluble protein fractions from the WT and Kv4.2 $^{-/-}$ brains were used for immunoprecipitations with 5 μg of an anti-Kv4.2 rabbit polyclonal antibody (Millipore). Protein A-magnetic beads (Invitrogen) were incubated with the protein samples and antibodies for 2 h at 4°C. Magnetic beads and bound antibodies were then collected and washed four times with ice-cold lysis buffer, and isolated protein complexes were eluted from the beads in 1× NuPAGE LDS sample buffer (Invitrogen). Samples were then fractionated by SDS-PAGE gels and transferred to PVDF membranes for immunoblotting as described above.

Protein lysates were prepared from HEK-293 cells harvested 24 h after transfections using ice-cold PBS containing 1% Triton and protease inhibitor (Complete mini EDTA *ad libitum* protease inhibitor mixture tablet from Roche) and processed for Western blot analysis described above for cortical samples.

Quantitative real-time PCR. For QRT-PCR experiments, posterior cortical samples were collected from WT, Kv4.2 $^{-/-}$, Kv4.3 $^{-/-}$, Kv4.2 $^{-/-}$/Kv4.3 $^{-/-}$, and KChIP3 $^{-/-}$ mice as described above. RNA was isolated from cortical samples and cDNA was produced using standard methods (Mullis and Faloona, 1987). Briefly, RNA was isolated by using the RNeasy mini kit from QIAGEN according the directions from the manufacturer, and RNA concentrations were determined by optical density measurements. Single-stranded cDNA was produced from 2 μg of total isolated RNA using the High Capacity cDNA Archive kit from Applied Biosystems. The expression levels of KChIP2, 3, and 4 were determined using sequence specific primers (see below) and SYBR Green (Applied Biosystems) for QRT-PCR; experiments were conducted on a 7900HT Fast Real-Time PCR System (Applied Biosystems). Data were analyzed using the threshold cycle relative quantification method, with GAPDH as

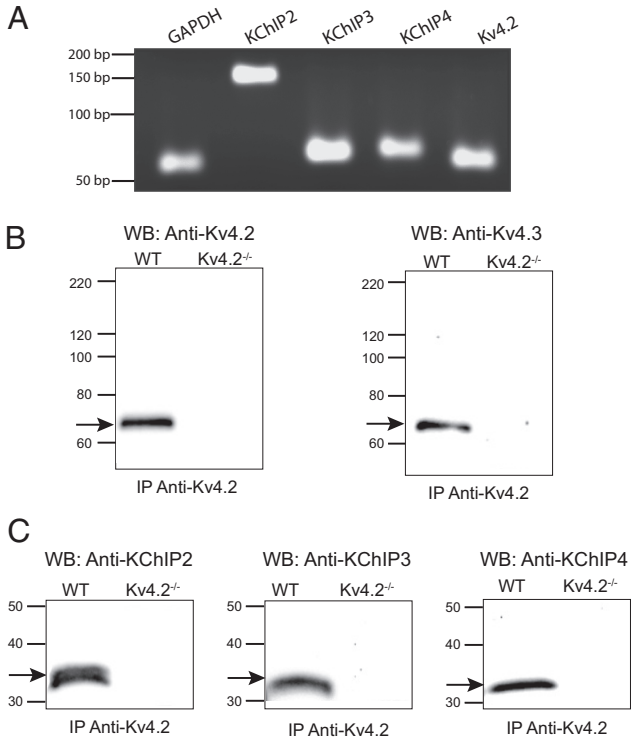

Figure 2. Expression of KChIP2, KChIP3, and KChIP4 in cortex and coimmunoprecipitation with Kv4.2. To examine the expression of KChIP transcripts, RNA was extracted from samples prepared from the posterior (~1 mm) cortex (containing visual cortex) of adult WT mice. ***A***, Using sequence-specific primer pairs and RT-PCR, transcripts coding for KChIP2, KChIP3, and KChIP4 were readily detected. Experiments were also performed to examine KChIP protein expression and association with Kv4.2. Immunoprecipitations using a rabbit anti-Kv4.2 antibody were conducted on lysates prepared from the posterior cortices of WT or Kv4.2 $^{-/-}$ mice, and blots of fractionated immunoprecipitated samples were probed using subunit-specific antibodies. ***B***, In immunoprecipitated samples from WT cortices, but not in those from Kv4.2 $^{-/-}$ cortices, both Kv4.2 and Kv4.3 were readily detected. ***C***, In immunoprecipitated samples from WT, but not Kv4.2 $^{-/-}$, cortices, KChIP2, KChIP3, and KChIP4 were also detected indicating that all three KChIP proteins are expressed and assemble with Kv4.2 in cortex. Molecular masses are indicated on the blots in kilodaltons.

the endogenous control. Primer sequences used to detect KChIP expression were as follows: KChIP2, forward, GGCTGTATCACGAAGGAGGAA; reverse, CCGTCCTTGTTTCTGTCCATC; KChIP3, forward, GGAGATCCTGGGCGCATAC; reverse, GTGAACCGTGGCCTTTGC; and KChIP4, forward, TGATCGTCATTGTGCTTTTTGTT; reverse, GCTGTCTTCTAAACCTGCTTCAATC.

Results

Disruption of KChIP3 expression decreases I_A density in cortical pyramidal neurons

The finding that expression of KChIP3 protein was markedly decreased in the cortices of mice harboring a targeted disruption of the *Kcnd2* (Kv4.2) locus (Nerbonne et al., 2008) suggested that KChIP3 may play an important role in the generation of functional Kv4-encoded I_A channels in cortical neurons. To explore this hypothesis, whole-cell Kv currents, evoked in response to steps to depolarized potentials (−40 through +40 mV in 10 mV increments) from a holding potential of −70 mV, were examined in cortical pyramidal neurons isolated from WT and KChIP3 $^{-/-}$ mice. The waveforms of the Kv currents recorded from WT (Fig. 1*A*) and KChIP3 $^{-/-}$ (Fig. 1*B*) neurons were similar, with prominent rapidly inactivating current components (I_A). To facilitate the quantification of I_A, Kv currents were also recorded from each cell using a prepulse paradigm (Fig. 1*A*, b; *B*, b) to inactivate I_A

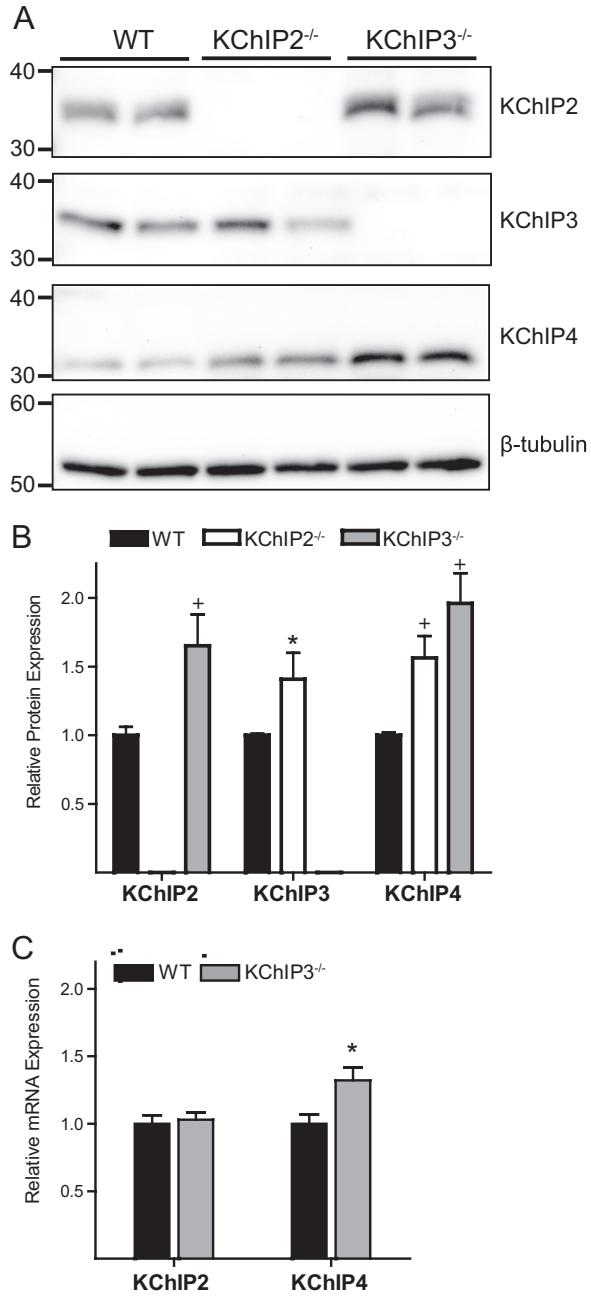

Figure 3. KChIPs are upregulated in KChIP2 $^{-/-}$ and KChIP3 $^{-/-}$ cortices. ***A***, Lysates prepared from the posterior (~1 mm) cortices of WT, KChIP2 $^{-/-}$, and KChIP3 $^{-/-}$ mice ($n = 6$ animals for each genotype) were fractionated, transferred to PVDF membranes, and probed with a specific anti-KChIP2, anti-KChIP3, or anti-KChIP4 antibody. All three KChIPs were detected in samples from WT mice. Confirming the specificities of the anti-KChIP2 and anti-KChIP3 antibodies, no signal was detected with the anti-KChIP2 or the anti-KChIP3 antibody in samples from KChIP2 $^{-/-}$ or KChIP3 $^{-/-}$ cortices, respectively. Blots were also probed with antibodies against β-tubulin to confirm equal loading of proteins. In each lane, anti-KChIP antibody signals were quantified and normalized to the anti-β-tubulin antibody signals. ***B***, In KChIP2 $^{-/-}$ cortices, the mean ± SEM expression levels of KChIP3 and KChIP4 proteins were significantly ($^{+}p < 0.01$) higher than in WT cortices. Similarly, the mean ± SEM expression levels of the KChIP2 and KChIP4 proteins were significantly ($^{*}p < 0.05$ and $^{+}p < 0.01$, respectively) higher in KChIP3 $^{-/-}$ cortices. ***C***, QRT-PCR analysis revealed that the mean ± SEM expression level of KChIP2 transcript was not significantly different in WT ($n = 6$) and KChIP3 $^{-/-}$ ($n = 6$) cortices, whereas the mean ± SEM expression level of KChIP4 transcript was slightly, but significantly ($^{*}p > 0.05$), higher in cortices from KChIP3 $^{-/-}$, compared with WT, mice. Molecular masses are indicated on the blots in kilodaltons.

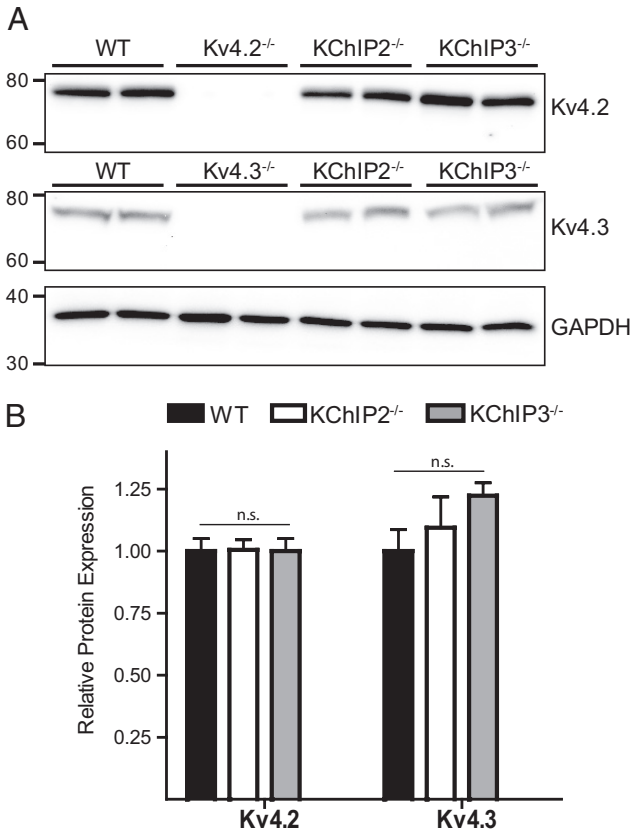

Figure 4. Maintained expression of Kv4.2 and Kv4.3 proteins in KChIP2 $^{-/-}$ and KChIP3 $^{-/-}$ cortices. ***A***, Lysates were prepared from the posterior (~1 mm) cortices of WT, KChIP2 $^{-/-}$, and KChIP3 $^{-/-}$ mice ($n = 6$ of each genotype) and fractionated by SDS-PAGE. After transfer, membranes were probed with a monoclonal anti-Kv4.2 or anit-Kv4.3 antibody and, subsequently, with an anti-GAPDH antibody, to verify equal loading of proteins in each lane. Signals from the anti-Kv4.2 and anti-Kv4.3 antibodies in each lane were quantified and normalized to signals from the anti-GAPDH antibody in the same lane. Molecular masses are indicated on the blots in kilodaltons. ***B***, Mean ± SEM levels of Kv4.2 and Kv4.3 proteins are not significantly different in either KChIP2 $^{-/-}$ or KChIP3 $^{-/-}$, compared with WT, cortices.

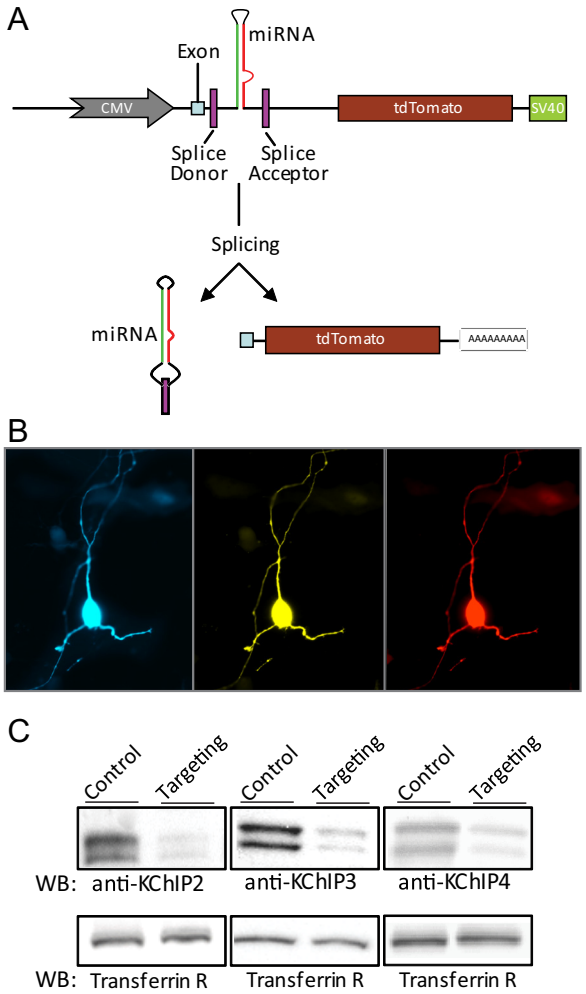

Figure 5. Validation of miRNA constructs to mediate RNAi based knockdown of KChIP2, KChIP3 or KChIP4 in neurons. As described in Materials and Methods, plasmids encoding human miR30, with substituted targeting sequences and a fluorescent protein (YFP, CFP, or tdTomato) on a single transcript, were generated. ***A***, The miR30 sequence was placed on an intron downstream of the CMV promoter and upstream of the sequence coding for the fluorescent protein (CFP, YFP, or tdTomato). ***B***, Transfections of these plasmids into neurons allowed for visual identification of neurons expressing one or all three of the plasmids for subsequent electrophysiological recording. ***C***, Specific sequences targeting KChIP2, KChIP3, and KChIP4 were screened in HEK-293 cells. The targeted KChIP (KChIP2, 3, or 4) was coexpressed with either a control (nontargeting) miRNA construct or with a miRNA construct containing sequence complementary to the sequence of the targeted KChIP. Lysates were prepared from transfected HEK-293 cells, fractionated by SDS-PAGE, transferred to membranes, and probed for KChIP2, KChIP3, or KChIP4. Blots were also probed with an anti-transferrin receptor (Transferrin R) antibody to verify equal loading of proteins. Targeting sequences found to reduce the expression of each of the targeted KChIPs are illustrated and were used in subsequent experiments, on cortical neurons.

selectively (Norris and Nerbonne, 2010); an additional 60 ms step to −10 mV was included before the depolarizing voltage steps (see paradigm illustrated in Fig. 1). Off-line subtraction of the records obtained using the prepulse paradigm from the control records (obtained from the same cell) allowed the isolation of I_A (Fig. 1*A*, a − b; *B*, a − b).

Analysis of I_A amplitudes in these subtracted records revealed that the mean ± SEM I_A density was modestly, but significantly ($p < 0.05$), lower in KChIP3 $^{-/-}$ ($n = 24$), compared with WT ($n = 22$), cortical pyramidal neurons (Fig. 1*C*). The voltage dependence of activation and the mean ± SEM τ of inactivation of the residual I_A in KChIP3 $^{-/-}$ neurons were not significantly different from the values determined for I_A in WT neurons (data not shown). Technically, changes in the voltage dependence of inactivation could also result in changes in I_A density. As described previously (Andreasen and Hablitz, 1992; Song et al., 1998; Wickenden et al., 1999), however, the presences of Cd^{2+} in the bath solution (to block Ca^{2+} channels) shifts the voltage dependence of activation and of steady-state inactivation of native I_A to more depolarized voltages. At −70 mV, the holding potential used in the experiments here, all of the I_A channels are available to be activated. The reduced I_A density in KChIP3 $^{-/-}$ pyramidal neurons, therefore, likely does not reflect a shift in I_A channel availability.

In addition to the rapidly inactivating I_A, previous studies (Locke and Nerbonne, 1997a,b; Yuan et al., 2005; Nerbonne et al., 2008; Norris and Nerbonne, 2010) have identified the presence of additional Kv currents in cortical pyramidal neurons: I_D, which inactivates more slowly than I_A (τ inactivation, ~250 ms); I_K, which inactivates very slowly (τ inactivation, ~2 s); and the noninactivating current, I_{SS}. Analysis of the decay phases of Kv currents in WT and KChIP3 $^{-/-}$ neurons revealed that, unlike I_A, the mean ± SEM amplitudes/densities of I_D, I_K, and I_{SS} were not significantly affected by the loss of KChIP3 (data not shown). The selective reduction of I_A in KChIP3 $^{-/-}$ cortical pyramidal neurons suggests that KChIP3 plays an important role in the gener-

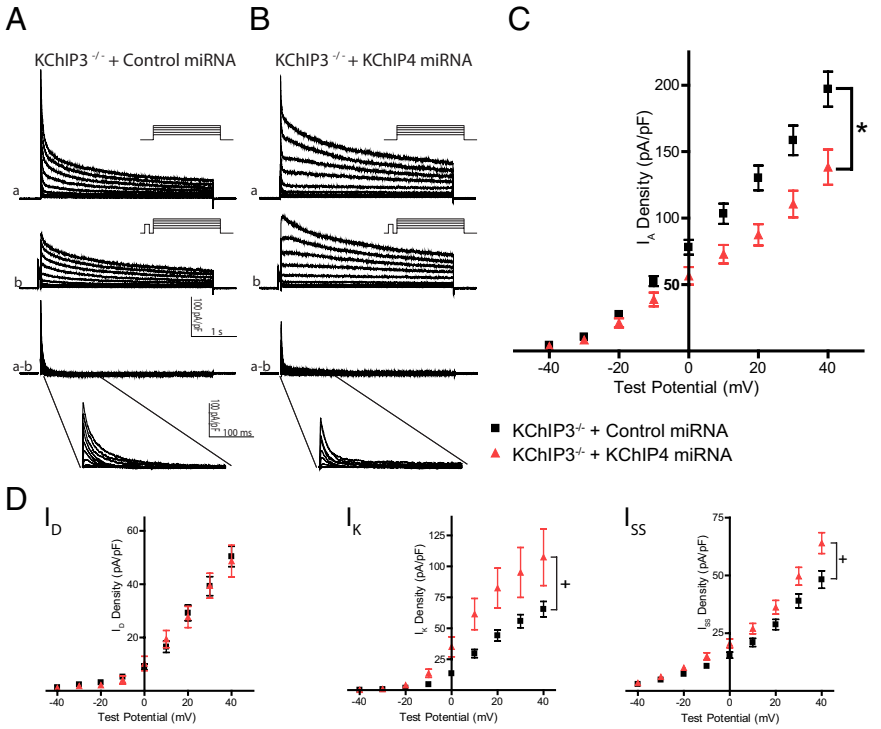

Figure 6. Knockdown of KChIP4 in KChIP3 $^{-/-}$ cortical pyramidal neurons results in decreased I_A density and upregulation of I_K and I_{SS}. ***A***, ***B***, Whole-cell Kv currents, elicited in response to depolarizing voltage steps, were recorded from transfected cortical pyramidal neurons isolated from KChIP3 $^{-/-}$ mice. Neurons were transfected by electroporation using the Amaxa Nucleofector system at the time of isolation with a miRNA construct containing either sequence targeting KChIP4 or a control nontargeting sequence; whole-cell recordings were obtained on the second and third days after transfections. I_A was isolated and quantified using the prepulse paradigm and off-line subtraction method described in the legend to Figure 1. ***C***, Analysis of the subtracted records (a − b) revealed that mean ± SEM I_A densities were significantly (*$p < 0.05$) lower in KChIP3 $^{-/-}$ neurons expressing miRNA targeting KChIP4 ($n = 16$) compared with KChIP3 $^{-/-}$ neurons expressing control miRNA ($n = 37$). ***D***, Analysis of the inactivation phases of the Kv currents also revealed that, in neurons expressing KChIP4 targeting miRNA, the mean ± SEM densities of I_K and I_{SS} were significantly ($^{+}p < 0.01$) higher than in control miRNA-expressing neurons.

ation and/or functioning of Kv4 channel complexes. The magnitude of I_A remaining in KChIP3 $^{-/-}$ cortical pyramidal neurons (Fig. 1*C*) also suggests that other KChIPs likely contribute to the generation of functional Kv4 channels. To examine the possible role of KChIP2, Kv current recordings were obtained from neurons isolated from mice (KChIP2 $^{-/-}$) harboring a targeted disruption of the gene (*Kcnip2*) encoding KChIP2 (Kuo et al., 2001). Analysis of the Kv currents using the prepulse paradigm described above, however, revealed that the mean ± SEM I_A density in KChIP2 $^{-/-}$ neurons ($n = 19$) was not significantly different from WT cells ($n = 22$) (not illustrated).

Coregulated expression of KChIP2, 3, and 4 in visual cortex

Previous studies have suggested that expression of KChIP1 is restricted to nonpyramidal interneurons in the cortex (Rhodes et al., 2004; Lein et al., 2007). As a result, KChIP1 was not considered in the analysis here. As illustrated in Figure 2*A*, mRNA transcripts encoding KChIP2, KChIP3, and KChIP4 were readily detected in RNA samples collected from the posterior (~1 mm) cortices of WT mice (see Material and Methods) consistent with previous reports examining KChIP expression in rodent brain (Rhodes et al., 2004; Xiong et al., 2004). Immunoprecipitation experiments using a rabbit anti-Kv4.2 antibody revealed that Kv4.2 was readily detected in fractionated protein samples from WT cortices, but not in samples from Kv4.2 $^{-/-}$ cortices. Also consistent with previous reports (Guo et al., 2002; Rhodes et al., 2004; Marionneau et al., 2009), Kv4.3 coimmunoprecipitated with Kv4.2 from WT cortical samples (Fig. 2*B*). No Kv4.3, however, was detected (Fig. 2*B*) in the samples from Kv4.2 $^{-/-}$ cortices, indicating that the anti-Kv4.2 antibody does not immunoprecipitate Kv4.3 in the absence of Kv4.2 and does not, therefore, cross-react with Kv4.3. KChIP2, KChIP3, and KChIP4 also coimmunoprecipitated with Kv4.2 from WT, but not Kv4.2 $^{-/-}$, cortical samples (Fig. 2*C*). The finding that KChIP2, KChIP3, and KChIP4 coimmunoprecipitate with Kv4.2 further suggests a role for each of these KChIPs in the generation of Kv4.2 channel complexes in cortical pyramidal neurons.

In parallel experiments, fractionated protein samples prepared from WT and KChIP3 $^{-/-}$ cortices ($n = 6$ animals for each genotype) were probed with specific anti-KChIP2, anti-KChIP3, and anti-KChIP4 antibodies (Fig. 3*A*). The signals from each anti-KChIP antibody were measured and normalized to the signal from the anti-β-tubulin antibody in the same lane. Quantitative analysis of multiple blots revealed that the mean ± SEM expression levels of both KChIP2 and KChIP4 were significantly ($p < 0.02$) higher in the KChIP3 $^{-/-}$, relative to the WT, samples (Fig. 3*B*). Parallel experiments on KChIP2 $^{-/-}$ cortical lysates revealed that the mean ± SEM protein levels of both KChIP3 and KChIP4 were significantly ($p < 0.002$) higher in KChIP2 $^{-/-}$ compared with WT, samples (Fig. 3*A*,*B*). To explore the role of transcriptional remodeling, RNA was isolated from the (posterior) cortices of KChIP3 $^{-/-}$ and WT mice ($n = 6$ for each genotype), and KChIP2 and KChIP4 transcript expression levels were examined. As illustrated in Figure 3*C*, the mean ± SEM expression level of the transcript encoding KChIP2 was similar in KChIP3 $^{-/-}$ and WT samples. The mean ± SEM level of KChIP4 transcript expression was significantly ($p < 0.05$) higher in KChIP3 $^{-/-}$, relative to WT cortices, although the magnitude (~30%) of the increase was much smaller than the twofold increase in KChIP4 protein expression.

Parallel experiments were completed to examine the expression levels of the Kv4.2 and Kv4.3 proteins in KChIP2 $^{-/-}$ and KChIP3 $^{-/-}$ cortices. In contrast to the marked changes in KChIP protein expression, analyses of Western blots on fractionated protein lysates prepared from the (posterior) cortices of KChIP2 $^{-/-}$, KChIP3 $^{-/-}$, and WT mice ($n = 6$ for each genotype) probed with specific antibodies against either Kv4.2 or Kv4.3 (Fig. 4*A*) revealed that the mean ± SEM expression levels of the Kv4.2 and Kv4.3 proteins were not significantly different in samples from KChIP2 $^{-/-}$ or KChIP3 $^{-/-}$, relative to WT, cortices (Fig. 4*B*).

miRNA-mediated RNAi knockdown of KChIP2, 3, and 4 expression

The biochemical experiments presented above suggest that the KChIPs are able to compensate for one another. An RNAi-based strategy was developed, therefore, to allow for the simultaneous knockdown of KChIP2, 3, and 4 expression in cortical pyramidal

neurons. Briefly, using a previously described approach (Du et al., 2006), plasmids encoding a targeting miRNA and a fluorescent protein (CFP, YFP, or tdtomato) were designed such that both components are present in a single transcript that is spliced apart and the components are processed separately (as illustrated in Fig. 5*A*). Separation of the miRNA and the fluorescent protein coding sequences by RNA splicing enhances the expression the fluorescent protein because the coding region is not degraded during the processing of the miRNA (Du et al., 2006), allowing for robust expression of the fluorophore as a faithful reporter of miRNA expression in transfected neurons. The miRNA plasmids described here allowed for the visual identification of transfected neurons expressing multiple miRNA constructs (as illustrated in Fig. 5*B*) for subsequent electrophysiological recordings.

Constructs containing individual sequences targeting KChIP2, KChIP3, or KChIP4 were cotransfected into HEK-293 cells with a plasmid encoding the targeted KChIP to identify sequences able to suppress the expression of each of the KChIPs. The effectiveness of each targeting sequence in reducing the expression of the targeted KChIP, compared with nontargeting control sequence, was assayed using Western blots performed on lysates prepared from transfected (HEK-293) cells. Of the individual sequences tested, those listed in Materials and Methods markedly suppressed the expression of KChIP2, KChIP3, or KChIP4 (Fig. 5*C*) and were used in subsequent experiments in neurons. Each of the miRNA sequences was specific to the targeted KChIP (i.e., none was complementary to mRNA sequences encoding KChIPs other than the targeted KChIP).

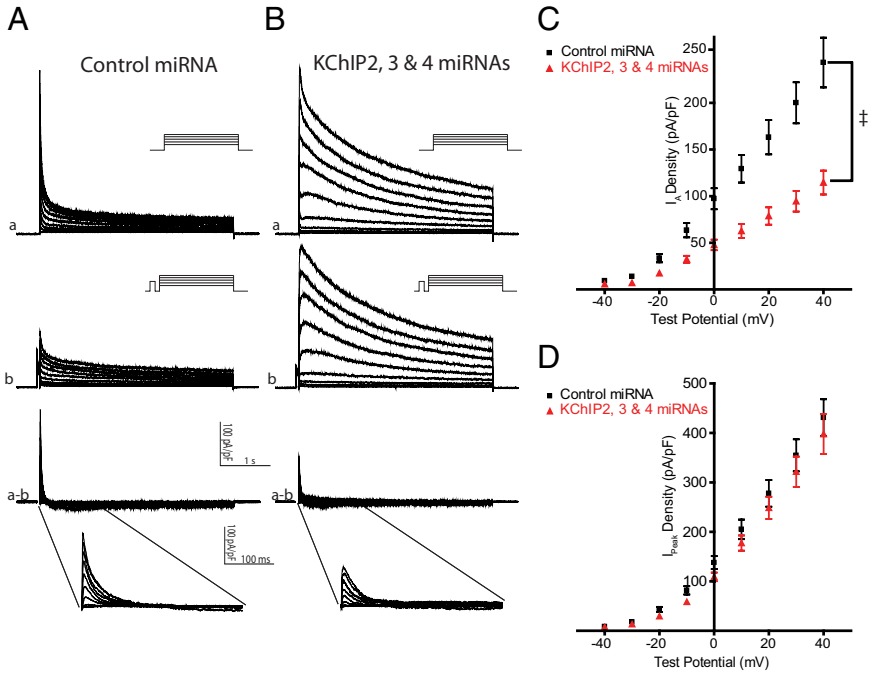

Figure 7. Concurrent knockdown of KChIP2, KChIP3, and KChIP4 in Kv1.4 $^{-/-}$ cortical pyramidal neurons results in marked reductions in Kv4-encoded I_A densities and K_V current remodeling. To examine the combined role(s) of the KChIPs in the generation of Kv4-encoded I_A channels, cortical pyramidal neurons were isolated from Kv1.4 $^{-/-}$ mice and transfected with the validated miRNA constructs targeting KChIP2, KChIP3, and KChIP4 or with plasmids containing control (nontargeting) sequences. Because each KChIP miRNA construct also encoded for a distinct fluorescent protein (CFP, YFP, or tdTomato), cells expressing all three KChIP targeting miRNA constructs could be identified. ***A***, ***B***, Recordings were obtained from neurons expressing control plasmids (***A***) or all three targeting plasmids (***B***). Surprisingly, no prominent rapidly inactivating component was observed in approximately one-half (11 of 20) of the neurons expressing the KChIP targeting miRNA constructs and delayed rectifier currents were increased. In all cells, I_A was isolated and quantified using the prepulse paradigm described in the legend to Figure 1. Analyses of subtracted records (a − b) revealed residual Kv4-encoded I_A in all neurons expressing the three KChIP targeting miRNAs simultaneously. The mean ± SEM I_A density was significantly ($^{\ddagger}p < 0.001$) lower (***C***) in neurons expressing the three KChIP targeting miRNA constructs ($n = 20$) than in neurons expressing control constructs ($n = 21$). ***D***, Consistent with the upregulation of delayed rectifier currents, analysis of the peak current (I_{Peak}) revealed no significant reduction in mean ± SEM I_{Peak} density in neurons expressing KChIP targeting miRNA compared with those expressing control constructs, despite the marked reduction in I_A densities (c).

Knockdown of KChIP4 expression in KChIP3 $^{-/-}$ neurons decreased I_A density

The finding that the KChIP4 protein is upregulated in KChIP3 $^{-/-}$ (and in KChIP2 $^{-/-}$) neurons (and may compensate for the loss of KChIP3 or KChIP2) was initially surprising because previous reports have suggested that KChIP4 acts to suppress, rather than promote, the surface expression of Kv4 channels (Shibata et al., 2003; Schwenk et al., 2008). To test directly the hypothesis that KChIP4 plays a role in the expression of functional Kv4-encoded I_A channels, Kv current recordings were obtained from KChIP3 $^{-/-}$ neurons transfected with a plasmid encoding either the control (nontargeting) miRNA (Fig. 6*A*) or the miRNA targeting KChIP4 (Fig. 6*B*). Parallel recordings were obtained from neurons expressing one (of the two) control nontargeting plasmids. One of these contained a scrambled targeting sequence ($n = 17$), and the other contained a control sequence targeting luciferase ($n = 20$). Analysis of the current records revealed no differences and the results were pooled.

Analysis of subtracted records (Fig. 6*A*,*B*, a − b) from KChIP3 $^{-/-}$ neurons transfected with control ($n = 37$) or KChIP4 targeting ($n = 16$) plasmids revealed that mean ± SEM I_A density was significantly ($p < 0.05$) lower in neurons expressing the KChIP4 targeting miRNA, compared with cells transfected with control miRNA (Fig. 6*C*). As illustrated in Figure 6*B*, the knockdown of KChIP4 in KChIP3 $^{-/-}$ neurons resulted in marked changes in the Kv current waveforms, changes reminiscent of those previously described in Kv4.2 $^{-/-}$ cortical pyramidal neurons (Nerbonne et al., 2008; Norris and Nerbonne, 2010). Analysis of the inactivation phases of the Kv currents revealed that the mean ± SEM amplitudes of the delayed rectifier currents, I_K and I_{SS}, were significantly ($p < 0.01$) larger in KChIP3 $^{-/-}$ neurons expressing the KChIP4 targeting miRNA, compared with KChIP3 $^{-/-}$ neurons transfected with control miRNA (Fig. 6*D*). In contrast, the mean ±SEM densities of I_D were not significantly different in control and KChIP4 targeting miRNA-expressing cells (Fig. 6*D*).

Attenuation of Kv4-encoded currents and remodeling of Kv currents with simultaneous knockdown of KChIP2, 3, and 4 in Kv1.4 $^{-/-}$ neurons

The results of the experiments described above suggest that KChIP2, KChIP3, and KChIP4 all contribute to the generation of functional of Kv4 channels and, in addition, that the KChIPs functionally compensate for one another. Experiments were undertaken, therefore, to examine the effects of concurrently

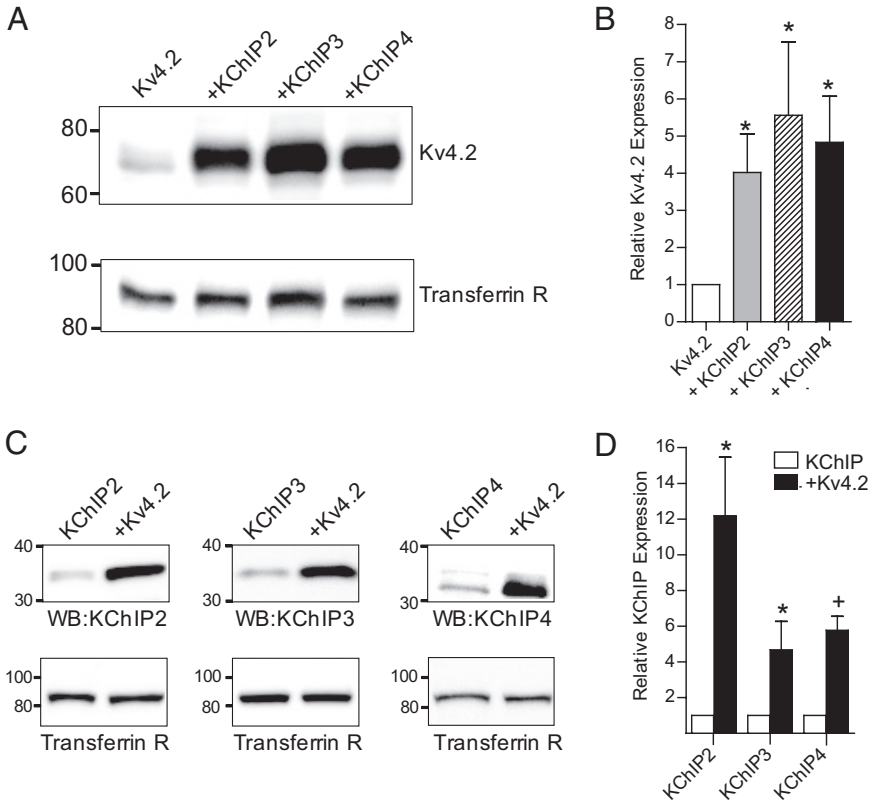

Figure 8. Coexpression of Kv4.2 with KChIP2, KChIP3, or KChIP4 results in the costabilization of both the Kv4.2 and KChIP proteins. HEK-293 cells were transfected with DNA constructs encoding Kv4.2 alone ($n = 9$), one of the KChIPs (KChIP2, $n = 6$; KChIP3, $n = 9$; KChIP4, $n = 6$) alone, or Kv4.2 in combination with KChIP2 ($n = 6$), KChIP3 ($n = 9$), or KChIP4 ($n = 6$). ***A***, Western blots on lysates prepared from transfected HEK-293 cells were probed with the monoclonal anti-Kv4.2 antibody. Blots were also probed with anti-transferrin receptor antibody (Transferrin R) to verify equal loading of proteins in each lane. The anti-Kv4.2 antibody signals were measured and normalized to the signals from the anti-transferrin receptor in the same lane. ***B***, Quantitative analyses revealed a significant ($^*p < 0.05$) increase in Kv4.2 protein in cells expressing Kv4.2 plus one of the three KChIPs, compared with cells expressing Kv4.2 alone. ***C***, Western blots conducted on HEK-293 cell lysates using the anti-KChIP2, anti-KChIP3, or anti-KChIP4 antibody also revealed that KChIP protein expression was increased in cells coexpressing Kv4.2, compared with cells expressing KChIP2, 3, or 4 alone. ***D***, Mean ± SEM levels of KChIP2, 3, and 4 protein expression were significantly ($^*p < 0.05$; $^+p < 0.01$) higher in cells coexpressing Kv4.2 compared with cells expressing either of the KChIP proteins alone.

knocking down the expression of KChIP2, 3, and 4 on Kv4-encoded I_A. These experiments were performed in neurons isolated from mice (Kv1.4$^{-/-}$) harboring a targeted disruption of the gene (*Kcna4*) encoding for Kv1.4 to allow for the analysis of effects on Kv4-encoded I_A without contamination from the Kv1.4-encoded component of I_A (Norris and Nerbonne, 2010). Whole-cell Kv current recordings were obtained from Kv1.4$^{-/-}$ neurons ($n = 20$) visually identified to be expressing the three miRNA constructs targeting KChIP2, 3, and 4 or neurons ($n = 21$) transfected with control plasmids (Fig. 7*A*,*B*). Analyses of the subtracted current records revealed residual Kv4-encoded I_A in all Kv1.4$^{-/-}$ neurons expressing the three KChIP targeting miRNA constructs. In addition, the voltage dependence of activation and the mean ± SEM τ of inactivation of the residual I_A (data not shown) were similar to values determined in WT neurons (see Discussion). The mean ± SEM I_A density, however, was significantly ($p < 0.001$) lower in Kv1.4$^{-/-}$ neurons expressing all three of KChIP targeting miRNA compared with Kv1.4$^{-/-}$ neurons expressing control constructs (Fig. 7*C*).

In addition to the marked reductions in I_A densities in the subtracted current records (a − b), the Kv current waveforms in Kv1.4$^{-/-}$ neurons expressing the KChIP targeting miRNAs were quite heterogeneous. In approximately one-half (11 of 20) of the Kv1.4$^{-/-}$ neurons expressing the KChIP targeting miRNAs, no prominent rapidly inactivating current component was evident and delayed rectifier Kv currents were increased (Fig. 7*B*) reminiscent of the Kv current waveforms in Kv4.2$^{-/-}$ neurons, in which upregulated I_K and I_{SS} mask the residual I_A (Nerbonne et al., 2008; Norris and Nerbonne, 2010). In the remaining Kv1.4$^{-/-}$ neurons expressing the KChIP targeting miRNAs (9 of 20), a rapidly inactivating component was clearly evident in the macroscopic Kv current waveforms (not illustrated). The marked alteration in the Kv current waveforms and the masking of the residual I_A component in many of the Kv1.4$^{-/-}$ neurons expressing the KChIP targeting miRNAs (Fig. 7*B*) suggests a greater upregulation in the amplitudes of I_K and I_{SS} than in KChIP3$^{-/-}$ neurons expressing the KChIP4 targeting miRNA (Fig. 6*D*). Consistent with remodeling of I_K and I_{SS}, mean ± SEM peak Kv current densities were not significantly different in neurons expressing the three KChIP targeting miRNA constructs, compared with those expressing control miRNA constructs (Fig. 7*D*), despite the marked decrease in mean I_A densities (Fig. 7*C*).

Expression of KChIP2, 3, and 4 proteins depends on the expression of Kv4 α-subunit proteins

The observed decreases in KChIP protein expression in Kv4.2$^{-/-}$ cortices (and other brain regions) suggest that KChIP protein expression is directly linked to Kv4.2 expression (Menegola and Trimmer, 2006; Nerbonne et al., 2008). To test this hypothesis directly, HEK-293 cells were transfected with DNA constructs encoding Kv4.2 alone, one of the KChIPs alone, or Kv4.2 and one of the KChIPs. As illustrated in Figure 8*A*, coexpression of Kv4.2 with KChIP2 ($n = 6$), KChIP3 ($n = 9$), or KChIP4 ($n = 6$) resulted in significant ($p < 0.05$) increases in mean ± SEM Kv4.2 protein levels (Fig. 8*B*) compared with cells ($n = 9$) expressing Kv4.2 alone. In addition, expression of Kv4.2 increased KChIP protein expression (Fig. 8*C*), and mean ± SEM KChIP2, KChIP3, and KChIP4 protein levels were significantly ($p < 0.05$) higher with coexpression of Kv4.2 compared with cells expressing each of the KChIPs alone (Fig. 8*D*).

To explore the hypothesis that the expression of the KChIP2, KChIP3, and KChIP4 proteins is linked to expression of the Kv4 α-subunit proteins in cortical neurons, Western blots on fractionated proteins from the posterior cortices of adult WT ($n = 6$), Kv4.2$^{-/-}$ ($n = 6$), Kv4.3$^{-/-}$ ($n = 6$), and Kv4.2$^{-/-}$/Kv4.3$^{-/-}$ ($n = 3$) mice were probed with antibodies specific for KChIP2, KChIP3, or KChIP4 (Fig. 9). Blots were subsequently probed with an anti-β-tubulin antibody to confirm equal loading of proteins in each lane. Quantitative analysis revealed that the mean ± SEM expression levels of the KChIP2, KChIP3, and KChIP4 proteins were significantly ($p < 0.01$) lower in Kv4.2$^{-/-}$ samples, compared with WT samples (Fig. 9*B*). Also, relative to WT sam-

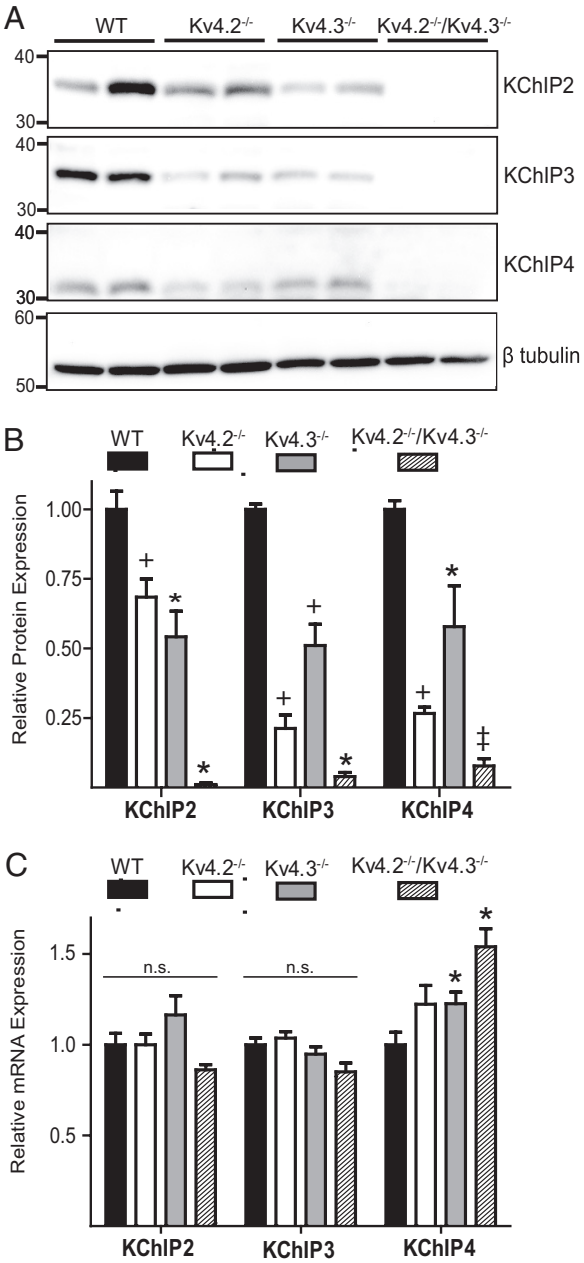

Figure 9. Endogenous KChIP2, KChIP3, and KChIP4 protein expression is dependent on the expression of Kv4 α-subunits. ***A***, Representative Western blots of fractionated lysates prepared from posterior (~1 mm) cortices of WT ($n = 6$), Kv4.2$^{-/-}$ ($n = 6$), Kv4.3$^{-/-}$ ($n = 6$), and Kv4.2$^{-/-}$/Kv4.3$^{-/-}$ ($n = 3$) mice were probed with the anti-KChIP antibodies. KChIP protein levels were differentially affected by the loss of Kv4.2 or Kv4.3, although drastic reductions in all three proteins were evident with the loss of both Kv4.2 and Kv4.3. For quantification, blots were also probed with an anti-β-tubulin antibody to confirm equal protein loading, in each lane, and signals from the anti-KChIP2, 3, or 4 antibodies were normalized against the signals from the anti-β-tubulin antibody in the same lane. ***B***, Analysis of mean (±SEM) normalized data revealed that the expression levels of KChIP2, KChIP3, and KChIP4 proteins in Kv4.2$^{-/-}$ and Kv4.3$^{-/-}$ cortices were significantly ($^{*}p < 0.05$, $^{+}p < 0.01$, or $^{\ddagger}p < 0.001$) lower than in WT cortices. In Kv4.2$^{-/-}$Kv4.3$^{-/-}$ cortices, KChIP2, KChIP3, and KChIP4 protein expression levels were extremely low. ***C***, QRT-PCR of analysis of RNA isolated from the posterior cortices of WT ($n = 6$), Kv4.2$^{-/-}$ ($n = 6$), Kv4.3$^{-/-}$ ($n = 6$), and Kv4.2$^{-/-}$/Kv4.3$^{-/-}$ ($n = 3$) mice revealed no reductions in KChIP transcripts. The mean ± SEM transcript expression level of KChIP4 was, however, significantly ($p < 0.05$) higher in Kv4.3$^{-/-}$ and in Kv4.2$^{-/-}$/Kv4.3$^{-/-}$, compared with WT, cortices.

ples, the mean ± SEM expression levels of the KChIP2, KChIP3, and KChIP4 proteins were significantly ($p < 0.01$) lower in Kv4.3$^{-/-}$ samples. In addition, when samples from Kv4.2$^{-/-}$/Kv4.3$^{-/-}$ animals were examined, the KChIP2, KChIP3, and KChIP4 proteins were barely detectable (Fig. 9).

In contrast, QRT-PCR analysis of RNA samples from posterior cortices of Kv4.2$^{-/-}$ ($n = 6$), Kv4.3$^{-/-}$ ($n = 6$), and Kv4.2$^{-/-}$/4.3$^{-/-}$ ($n = 3$) mice revealed that the mean expression levels of the KChIP2, KChIP3, or KChIP4 transcripts were not lower in any of the genotypes relative to WT cortices. In fact, the only significant ($p < 0.05$) changes observed were increased (mean ± SEM) KChIP4 transcript expression in both the Kv4.3$^{-/-}$ and Kv4.2$^{-/-}$/Kv4.3$^{-/-}$ samples (Fig. 9*C*). In contrast to the near-complete loss of the KChIP2, KChIP3, and KChIP4 proteins in the Kv4.2$^{-/-}$/Kv4.3$^{-/-}$ cortices, there were no significant changes in mean ± SEM KChIP2 or KChIP3 transcript expression levels. The dramatic decreases in the expression levels of the KChIP proteins resulting from the disruption of Kv4.2 and/or Kv4.3 without corresponding decreases in mRNA levels are consistent with an important role for posttranscriptional mechanisms in the coupling between the expression of the KChIPs and the expression of the Kv4.2 and Kv4.3 α-subunits.

Discussion

KChIP2, KChIP3, and KChIP4 are critical components of functional Kv4 channel complexes in cortical pyramidal neurons

The results of the biochemical, molecular genetic, and electrophysiological experiments described here suggest that KChIP2, KChIP3, and KChIP4 are critical for the formation of functional Kv4 channel complexes in (mouse visual) cortical pyramidal neurons. All three KChIPs are robustly expressed in posterior cortex and, in addition, coimmunoprecipitate with Kv4.2 (Fig. 2). The results of the experiments completed here further indicate that the KChIPs can functionally compensate for one another. Specifically, the protein expression levels of the unperturbed KChIPs were upregulated in the cortices of KChIP2$^{-/-}$ and KChIP3$^{-/-}$ mice (Fig. 3), and I_A densities were either not (KChIP2$^{-/-}$) or only modestly (KChIP3$^{-/-}$) affected (Fig. 1). Additional experiments revealed, however, that the simultaneous RNAi-mediated reduction in the expression of KChIP2, KChIP3, and KChIP4 resulted in marked reductions in Kv4-encoded I_A densities (Fig. 7). Perhaps not surprisingly, I_A was not completely eliminated in the Kv1.4$^{-/-}$ neurons expressing the three KChIP targeting miRNA constructs, consistent with residual KChIP protein, likely reflecting incomplete knockdown of KChIP2, 3, and/or 4 expression.

Expression of KChIP proteins is dependent on the expression of Kv4 α-subunits

The results of the experiments detailed here also revealed that the expression of the KChIP2, KChIP3, and KChIP4 proteins is dependent on the expression of Kv4 α-subunits in cortical tissue. Consistent with previous reports that KChIP2 and KChIP3 expression is decreased in Kv4.2$^{-/-}$ hippocampal neurons (Menegola and Trimmer, 2006), the results here demonstrate that protein expression levels of KChIP2, KChIP3, and KChIP4 are decreased in the cortices of Kv4.2$^{-/-}$mice. Reduced expression of the KChIP2, 3, and 4 proteins was also observed in cortical samples from Kv4.3$^{-/-}$ mice. Additionally, all three KChIP proteins were barely detectable in Kv4.2$^{-/-}$/Kv4.3$^{-/-}$ cortices (Fig. 9). Importantly, the marked reductions in the expression levels of KChIP proteins do not reflect changes in transcript levels (Fig.

9*C*), suggesting that posttranslational mechanisms are responsible for the loss of KChIP proteins in Kv4.2$^{-/-}$, Kv4.3$^{-/-}$, and Kv4.2$^{-/-}$/Kv4.3$^{-/-}$ neurons.

Previous reports indicate that the KChIPs interact with Kv4 α-subunits early during channel biogenesis (Hasdemir et al., 2005; Flowerdew and Burgoyne, 2009). The results of experiments presented here suggest that, when the KChIP and Kv4 α-subunits bind, the proteins are stabilized, leading to increased levels of both the Kv4 α-subunit and accessory KChIP proteins (Fig. 8). The observed increases in the protein expression levels of the remaining KChIP proteins in KChIP2$^{-/-}$ and KChIP3$^{-/-}$ cortices (Fig. 3) suggest that, when the expression of an individual KChIP is disrupted, the remaining KChIP proteins are stabilized by binding to available Kv4 α-subunits, resulting in net increases in the nondisrupted KChIP proteins. Interestingly, the codependence of the expression of Kv α- and accessory subunit proteins has been previously reported in studies using *Caenorhabditis elegans* (Bianchi et al., 2003) and *Drosophila* (Wu et al., 2010), suggesting that the mechanisms linking accessory and α-subunits expression are highly conserved.

Functions of KChIP2, 3, and 4

Interestingly, results from several recent studies suggest that individual KChIPs may interact with specific signaling molecules (e.g., PKA or PKC) to regulate the modulation of Kv4 channels by specific signaling pathways (Schrader et al., 2002; Lin et al., 2010). Additional diversity of KChIP function may originate from splice variants of the individual KChIP genes. Splice variants of KChIP2 and KChIP4, for example, have been described to promote surface expression of heterologously expressed Kv4 α-subunits, and other variants have been reported to have inhibitory effects on the surface expression of Kv4 α-subunits (Shibata et al., 2003; Decher et al., 2004). It was also recently reported that KChIP3 (but not other KChIPs) functions as a Ca^{2+} sensor to modulate the voltage dependence of inactivation of Kv4-encoded I_A in response to the entry of Ca^{2+} through Cav3-encoded voltage-gated Ca^{2+} channels (Anderson et al., 2010a,b). The findings presented here raise the interesting possibility that KChIP2 and KChIP4, in addition to KChIP3, also participate in the generation and functioning of distinct Kv4 channel complexes in cortical pyramidal neurons. Future experiments designed to explore this hypothesis are necessary to determine the unique roles of each of the individual KChIPs.

The results presented here, which indicate that multiple KChIPs are concurrently involved in the generation and function of Kv4 channels, highlight the molecular diversity that likely exists in Kv4 channel complexes in neurons. One Kv4 channel complex could, for example, be formed by a heterometric complex of Kv4.2 and Kv4.3 α-subunits bound simultaneously to multiple different KChIPs. In the same cell, another Kv4 channel complex could be formed by a homomultimer of Kv4.2 α-subunits with a single type of KChIP. As suggested previously, considerable evidence supports the additional inclusion of DPP6 and/or DPP10 subunits, as well as Kvβ subunits in the generation and/or functioning of Kv4 channel complexes (Nadal et al., 2003; Aimond et al., 2005; Jerng et al., 2005; Marionneau et al., 2009), thus exponentially diversifying the possible protein combinations that may be present in native neuronal Kv4 channel complexes. This molecular diversity may provide for high-resolution regulatory mechanisms for fine-tuning neuronal excitability and neuronal computations.

In addition to playing crucial roles as Kv4 channel accessory subunits, KChIPs have been shown to play important roles in other cellular processes (Buxbaum, 2004; Sours-Brothers et al., 2009). Notably, KChIP3, also called calsenilin (Buxbaum et al., 1998) and downstream regulatory element antagonist modulator (DREAM) (Carrión et al., 1999), has also been shown to modulate γ-secretase activity (Lilliehook et al., 2003), to alter gene transcription, and to function in apoptosis (Jo et al., 2001). Recently, it was reported that KChIP3/DREAM also modulates the NMDA class glutamate receptors in hippocampal neurons (Zhang et al., 2010). It is not clear how these (or other possible) functions of the KChIPs can be reconciled with the results presented here or with previously published results (Menegola and Trimmer, 2006), which clearly suggest that the expression of the KChIP proteins depends directly on the expression of Kv4 channel α-subunits. The possibility the KChIPs, particularly KChIP3, may coordinate the regulation of channel function with other cellular processes is an intriguing possibility that merits additional consideration and direct evaluation.

Remodeling of Kv currents after the disruption of KChIP expression

Remodeling of Kv currents was evident in KChIP3$^{-/-}$ neurons expressing KChIP4 targeting miRNA (Fig. 6) and in Kv1.4$^{-/-}$ neurons expressing miRNAs targeting KChIP2, 3, and 4 (Fig. 7). The upregulation of the I_K and I_{SS} components observed when the expression of multiple KChIPs was simultaneously disrupted is similar to the remodeling evident in Kv4.2$^{-/-}$, Kv4.3$^{-/-}$, and Kv4.2$^{-/-}$/Kv4.3$^{-/-}$ cortical pyramidal neurons previously reported (Nerbonne et al., 2008; Norris and Nerbonne, 2010). Interestingly, no remodeling of Kv currents was evident in response to the loss of Kv4-encoded I_A by the expression of a dominant-negative Kv4 construct in (rat) cortical pyramidal neurons (Yuan et al., 2005), suggesting that the mechanisms mediating the remodeling of ionic currents are based on protein expression rather than changes in the electrical properties of the neurons. A similar conclusion was reached in previous studies on lobster pyloric neurons, in which it was demonstrated that the overexpression of wild-type Kv4 α-subunits (which increased Kv4-encoded I_A) or expression of a inactive Kv4 mutant protein resulted in increased density of the hyperpolarization activated current, I_h (MacLean et al., 2003). Together, the remodeling of Kv currents evident in response to the disruption of the expression of multiple KChIPs and the finding of decreased expression levels of KChIP proteins in samples from Kv4.2$^{-/-}$ mice suggests that the KChIPs, through direct or indirect effects, may play important roles in balancing the expression of ionic conductances in cortical pyramidal neurons. Clearly, future experiments aimed at exploring this possibility will be of considerable interest.

References

Aghajanian GK (1985) Modulation of a transient outward current in serotonergic neurones by alpha 1-adrenoceptors. Nature 315:501–503.

Aimond F, Kwak SP, Rhodes KJ, Nerbonne JM (2005) Accessory Kvbeta1 subunits differentially modulate the functional expression of voltage-gated K^+ channels in mouse ventricular myocytes. Circ Res 96:451–458.

Alexander JC, McDermott CM, Tunur T, Rands V, Stelly C, Karhson D, Bowlby MR, An WF, Sweatt JD, Schrader LA (2009) The role of calsenilin/DREAM/KChIP3 in contextual fear conditioning. Learn Mem 16:167–177.

An WF, Bowlby MR, Betty M, Cao J, Ling HP, Mendoza G, Hinson JW, Mattsson KI, Strassle BW, Trimmer JS, Rhodes KJ (2000) Modulation of A-type potassium channels by a family of calcium sensors. Nature 403:553–556.

Anderson D, Rehak R, Hameed SW, Hamish M, Zamponi GW, Turner RW (2010a) Regulation of the KV4.2 complex by CaV3.1 calcium channels. Channels (Austin) 4:163–167.

Anderson D, Mehaffey WH, Iftinca M, Rehak R, Engbers JD, Hameed S, Zamponi GW, Turner RW (2010b) Regulation of neuronal activity by Cav3-Kv4 channel signaling complexes. Nat Neurosci 13:333–337.

Andreasen M, Hablitz JJ (1992) Kinetic properties of a transient outward current in rat neocortical neurons. J Neurophysiol 68:1133–1142.

Bernard C, Anderson A, Becker A, Poolos NP, Beck H, Johnston D (2004) Acquired dendritic channelopathy in temporal lobe epilepsy. Science 305:532–535.

Bianchi L, Kwok SM, Driscoll M, Sesti F (2003) A potassium channel-MiRP complex controls neurosensory function in *Caenorhabditis elegans*. J Biol Chem 278:12415–12424.

Bothwell AL, Paskind M, Reth M, Imanishi-Kari T, Rajewsky K, Baltimore D (1981) Heavy chain variable region contribution to the NPb family of antibodies: somatic mutation evident in a gamma 2a variable region. Cell 24:625–637.

Bourdeau ML, Morin F, Laurent CE, Azzi M, Lacaille JC (2007) Kv4.3-mediated A-type K^+ currents underlie rhythmic activity in hippocampal interneurons. J Neurosci 27:1942–1953.

Brondyk WH (1995) The pCI-neo mammalian expression vector. Promega Notes 51:10–14.

Brunet S, Aimond F, Li H, Guo W, Eldstrom J, Fedida D, Yamada KA, Nerbonne JM (2004) Heterogeneous expression of repolarizing, voltage-gated K^+ currents in adult mouse ventricles. J Physiol 559:103–120.

Buxbaum JD (2004) A role for calsenilin and related proteins in multiple aspects of neuronal function. Biochem Biophys Res Commun 322:1140–1144.

Buxbaum JD, Choi EK, Luo Y, Lilliehook C, Crowley AC, Merriam DE, Wasco W (1998) Calsenilin: a calcium-binding protein that interacts with the presenilins and regulates the levels of a presenilin fragment. Nat Med 4:1177–1181.

Cai X, Liang CW, Muralidharan S, Kao JP, Tang CM, Thompson SM (2004) Unique roles of SK and Kv4.2 potassium channels in dendritic integration. Neuron 44:351–364.

Carrión AM, Link WA, Ledo F, Mellström B, Naranjo JR (1999) DREAM is a Ca^{2+}-regulated transcriptional repressor. Nature 398:80–84.

Chen X, Yuan LL, Zhao C, Birnbaum SG, Frick A, Jung WE, Schwarz TL, Sweatt JD, Johnston D (2006) Deletion of Kv4.2 gene eliminates dendritic A-type K^+ current and enhances induction of long-term potentiation in hippocampal CA1 pyramidal neurons. J Neurosci 26: 12143–12151.

Connor JA, Stevens CF (1971a) Inward and delayed outward membrane currents in isolated neural somata under voltage clamp. J Physiol 213:1–19.

Connor JA, Stevens CF (1971b) Voltage clamp studies of a transient outward membrane current in gastropod neural somata. J Physiol 213:21–30.

Covarrubias M, Bhattacharji A, De Santiago-Castillo JA, Dougherty K, Kaulin YA, Na-Phuket TR, Wang G (2008) The neuronal Kv4 channel complex. Neurochem Res 33:1558–1567.

Decher N, Barth AS, Gonzalez T, Steinmeyer K, Sanguinetti MC (2004) Novel KChIP2 isoforms increase functional diversity of transient outward potassium currents. J Physiol 557:761–772.

Du G, Yonekubo J, Zeng Y, Osisami M, Frohman MA (2006) Design of expression vectors for RNA interference based on miRNAs and RNA splicing. FEBS J 273:5421–5427.

Flowerdew SE, Burgoyne RD (2009) A VAMP7/Vti1a SNARE complex distinguishes a non-conventional traffic route to the cell surface used by KChIP1 and Kv4 potassium channels. Biochem J 418:529–540.

Guo W, Li H, Aimond F, Johns DC, Rhodes KJ, Trimmer JS, Nerbonne JM (2002) Role of heteromultimers in the generation of myocardial transient outward K^+ currents. Circ Res 90:586–593.

Guo W, Jung WE, Marionneau C, Aimond F, Xu H, Yamada KA, Schwarz TL, Demolombe S, Nerbonne JM (2005) Targeted deletion of Kv4.2 eliminates $I_{to,f}$ and results in electrical and molecular remodeling, with no evidence of ventricular hypertrophy or myocardial dysfunction. Circ Res 97:1342–1350.

Hasdemir B, Fitzgerald DJ, Prior IA, Tepikin AV, Burgoyne RD (2005) Traffic of Kv4 K^+ channels mediated by KChIP1 is via a novel post-ER vesicular pathway. J Cell Biol 171:459–469.

Holmqvist MH, Cao J, Hernandez-Pineda R, Jacobson MD, Carroll KI, Sung MA, Betty M, Ge P, Gilbride KJ, Brown ME, Jurman ME, Lawson D, Silos-Santiago I, Xie Y, Covarrubias M, Rhodes KJ, Distefano PS, An WF (2002) Elimination of fast inactivation in Kv4 A-type potassium channels by an auxiliary subunit domain. Proc Natl Acad Sci U S A 99: 1035–1040.

Hu HJ, Carrasquillo Y, Karim F, Jung WE, Nerbonne JM, Schwarz TL, Gereau RW 4th (2006) The Kv4.2 potassium channel subunit is required for pain plasticity. Neuron 50:89–100.

Huettner JE, Baughman RW (1986) Primary culture of identified neurons from the visual cortex of postnatal rats. J Neurosci 6:3044–3060.

Jerng HH, Kunjilwar K, Pfaffinger PJ (2005) Multiprotein assembly of Kv4.2, KChIP3 and DPP10 produces ternary channel complexes with ISA-like properties. J Physiol 568:767–788.

Jo DG, Kim MJ, Choi YH, Kim IK, Song YH, Woo HN, Chung CW, Jung YK (2001) Pro-apoptotic function of calsenilin/DREAM/KChIP3. FASEB J 15:589–591.

Kuo HC, Cheng CF, Clark RB, Lin JJ, Lin JL, Hoshijima M, Nguyêñ-Trân VT, Gu Y, Ikeda Y, Chu PH, Ross J, Giles WR, Chien KR (2001) A defect in the Kv channel-interacting protein 2 (KChIP2) gene leads to a complete loss of I_{to} and confers susceptibility to ventricular tachycardia. Cell 107:801–813.

Lein ES, Hawrylycz MJ, Ao N, Ayres M, Bensinger A, Bernard A, Boe AF, Boguski MS, Brockway KS, Byrnes EJ, Chen L, Chen TM, Chin MC, Chong J, Crook BE, Czaplinska A, Dang CN, Datta S, Dee NR, Desaki AL, et al. (2007) Genome-wide atlas of gene expression in the adult mouse brain. Nature 445:168–176.

Lilliehook C, Bozdagi O, Yao J, Gomez-Ramirez M, Zaidi NF, Wasco W, Gandy S, Santucci AC, Haroutunian V, Huntley GW, Buxbaum JD (2003) Altered Aβ formation and long-term potentiation in a calsenilin knock-out. J Neurosci 23:9097–9106.

Lin L, Sun W, Wikenheiser AM, Kung F, Hoffman DA (2010) KChIP4a regulates Kv4.2 channel trafficking through PKA phosphorylation. Mol Cell Neurosci 43:315–325.

Locke RE, Nerbonne JM (1997a) Three kinetically distinct Ca^{2+}-independent depolarization-activated K^+ currents in callosal-projecting rat visual cortical neurons. J Neurophysiol 78:2309–2320.

Locke RE, Nerbonne JM (1997b) Role of voltage-gated K^+ currents in mediating the regular-spiking phenotype of callosal-projecting rat visual cortical neurons. J Neurophysiol 78:2321–2335.

MacLean JN, Zhang Y, Johnson BR, Harris-Warrick RM (2003) Activity-independent homeostasis in rhythmically active neurons. Neuron 37:109–120.

Maffie J, Rudy B (2008) Weighing the evidence for a ternary protein complex mediating A-type K^+ currents in neurons. J Physiol 586:5609–5623.

Makara JK, Losonczy A, Wen Q, Magee JC (2009) Experience-dependent compartmentalized dendritic plasticity in rat hippocampal CA1 pyramidal neurons. Nat Neurosci 12:1485–1487.

Marionneau C, Leduc RD, Rohrs HW, Link AJ, Townsend RR, Nerbonne JM (2009) Proteomic analyses of native brain K_V4.2 channel complexes. Channels (Austin) 3:284–294.

Martens JR, Kwak YG, Tamkun MM (1999) Modulation of Kv channel alpha/beta subunit interactions. Trends Cardiovasc Med 9:253–258.

Menegola M, Trimmer JS (2006) Unanticipated region- and cell-specific downregulation of individual KChIP auxiliary subunit isotypes in Kv4.2 knock-out mouse brain. J Neurosci 26:12137–12142.

Morohashi Y, Hatano N, Ohya S, Takikawa R, Watabiki T, Takasugi N, Imaizumi Y, Tomita T, Iwatsubo T (2002) Molecular cloning and characterization of CALP/KChIP4, a novel EF-hand protein interacting with presenilin 2 and voltage-gated potassium channel subunit Kv4. J Biol Chem 277:14965–14975.

Mullis KB, Faloona FA (1987) Specific synthesis of DNA in vitro via a polymerase-catalyzed chain reaction. Methods Enzymol 155:335–350.

Nadal MS, Ozaita A, Amarillo Y, Vega-Saenz de Miera E, Ma Y, Mo W, Goldberg EM, Misumi Y, Ikehara Y, Neubert TA, Rudy B (2003) The CD26-related dipeptidyl aminopeptidase-like protein DPPX is a critical component of neuronal A-type K^+ channels. Neuron 37:449–461.

Nerbonne JM, Gerber BR, Norris A, Burkhalter A (2008) Electrical remodelling maintains firing properties in cortical pyramidal neurons lacking KCND2-encoded A-type K^+ currents. J Physiol 586:1565–1579.

Niwa N, Wang W, Sha Q, Marionneau C, Nerbonne JM (2008) Kv4.3 is not required for the generation of functional $I_{to,f}$ channels in adult mouse ventricles. J Mol Cell Cardiol 44:95–104.

Norris AJ, Nerbonne JM (2010) Molecular dissection of I_A in cortical pyramidal neurons reveals three distinct components encoded by Kv4.2, Kv4.3, and Kv1.4 alpha-subunits. J Neurosci 30:5092–5101.

Olson A, Sheth N, Lee JS, Hannon G, Sachidanandam R (2006) RNAi Codex: a portal/database for short-hairpin RNA (shRNA) gene-silencing constructs. Nucleic Acids Res 34:D153–D157.

Patton C, Thompson S, Epel D (2004) Some precautions in using chelators to buffer metals in biological solutions. Cell Calcium 35:427–431.

Phuket TR, Covarrubias M (2009) Kv4 channels underlie the subthreshold-operating A-type K-current in nociceptive dorsal root ganglion neurons. Front Mol Neurosci 2:3.

Radicke S, Cotella D, Graf EM, Banse U, Jost N, Varró A, Tseng GN, Ravens U, Wettwer E (2006) Functional modulation of the transient outward current I_{to} by KCNE beta-subunits and regional distribution in human non-failing and failing hearts. Cardiovasc Res 71:695–703.

Rhodes KJ, Carroll KI, Sung MA, Doliveira LC, Monaghan MM, Burke SL, Strassle BW, Buchwalder L, Menegola M, Cao J, An WF, Trimmer JS (2004) KChIPs and Kv4 alpha subunits as integral components of A-type potassium channels in mammalian brain. J Neurosci 24:7903–7915.

Roepke TK, Kontogeorgis A, Ovanez C, Xu X, Young JB, Purtell K, Goldstein PA, Christini DJ, Peters NS, Akar FG, Gutstein DE, Lerner DJ, Abbott GW (2008) Targeted deletion of kcne2 impairs ventricular repolarization via disruption of $I_{K,slow1}$ and $I_{to,f}$. FASEB J 22:3648–3660.

Rogawski MA (1985) The A-current—how ubiquitous a feature of excitable cells is it. Trends Neurosci 8:214–219.

Schrader LA, Anderson AE, Mayne A, Pfaffinger PJ, Sweatt JD (2002) PKA modulation of Kv4.2-encoded A-type potassium channels requires formation of a supramolecular complex. J Neurosci 22:10123–10133.

Schulte U, Thumfart JO, Klöcker N, Sailer CA, Bildl W, Biniossek M, Dehn D, Deller T, Eble S, Abbass K, Wangler T, Knaus HG, Fakler B (2006) The epilepsy-linked Lgi1 protein assembles into presynaptic Kv1 channels and inhibits inactivation by Kvbeta1. Neuron 49:697–706.

Schwenk J, Zolles G, Kandias NG, Neubauer I, Kalbacher H, Covarrubias M, Fakler B, Bentrop D (2008) NMR analysis of KChIP4a reveals structural basis for control of surface expression of Kv4 channel complexes. J Biol Chem 283:18937–18946.

Shaner NC, Campbell RE, Steinbach PA, Giepmans BN, Palmer AE, Tsien RY (2004) Improved monomeric red, orange and yellow fluorescent proteins derived from Discosoma sp. red fluorescent protein. Nat Biotechnol 22:1567–1572.

Shibata R, Misonou H, Campomanes CR, Anderson AE, Schrader LA, Doliveira LC, Carroll KI, Sweatt JD, Rhodes KJ, Trimmer JS (2003) A fundamental role for KChIPs in determining the molecular properties and trafficking of Kv4.2 potassium channels. J Biol Chem 278:36445–36454.

Song WJ, Tkatch T, Baranauskas G, Ichinohe N, Kitai ST, Surmeier DJ (1998) Somatodendritic depolarization-activated potassium currents in rat neostriatal cholinergic interneurons are predominantly of the A type and attributable to coexpression of Kv4.2 and Kv4.1 subunits. J Neurosci 18:3124–3137.

Sours-Brothers S, Ma R, Koulen P (2009) Ca^{2+}-sensitive transcriptional regulation: direct DNA interaction by DREAM. Front Biosci 14:1851–1856.

Stegmeier F, Hu G, Rickles RJ, Hannon GJ, Elledge SJ (2005) A lentiviral microRNA-based system for single-copy polymerase II-regulated RNA interference in mammalian cells. Proc Natl Acad Sci U S A 102: 13212–13217.

Wickenden AD, Tsushima RG, Losito VA, Kaprielian R, Backx PH (1999) Effect of Cd2+ on Kv4.2 and Kv1.4 expressed in *Xenopus* oocytes and on the transient outward currents in rat and rabbit ventricular myocytes. Cell Physiol Biochem 9:11–28.

Wu MN, Joiner WJ, Dean T, Yue Z, Smith CJ, Chen D, Hoshi T, Sehgal A, Koh K (2010) SLEEPLESS, a Ly-6/neurotoxin family member, regulates the levels, localization and activity of Shaker. Nat Neurosci 13:69–75.

Xiong H, Kovacs I, Zhang Z (2004) Differential distribution of KChIPs mRNAs in adult mouse brain. Brain Res Mol Brain Res 128:103–111.

Yang EK, Alvira MR, Levitan ES, Takimoto K (2001) Kvbeta subunits increase expression of Kv4.3 channels by interacting with their C termini. J Biol Chem 276:4839–4844.

Yuan W, Burkhalter A, Nerbonne JM (2005) Functional role of the fast transient outward K^+ current I_A in pyramidal neurons in (rat) primary visual cortex. J Neurosci 25:9185–9194.

Zhang Y, Su P, Liang P, Liu T, Liu X, Liu XY, Zhang B, Han T, Zhu YB, Yin DM, Li J, Zhou Z, Wang KW, Wang Y (2010) The DREAM protein negatively regulates the NMDA receptor through interaction with the NR1 subunit. J Neurosci 30:7575–7586.